Study and Design of the Microstrip Patch Antenna Operating at 120 GHz

Salah-Eddine Didi, Imane Halkhams, Mohammed Fattah, Younes Balboul, Said Mazer, Moulhime EL Bekkali, and Sudipta Das

Abstract In this chapter, we will present a study concerning the design of a microstrip patch antenna with a rectangular slot intended for the wireless technology terahertz. This antenna operates for a frequency located in the terahertz band (120 GHz). The designed slot allows improving the characteristics of the antenna. The dimensions of this type of antenna for the terahertz band are reduced compared to conventional antennas. The patch and feeder cable sizes are small and difficult to manufacture. In this paper, we use a three-dimensional high-frequency structure simulator (HFSS) tool. The substrate chosen for this design is the rubber hard one with permittivity $\varepsilon r = 3$ and its height ($h = 0.1$ mm). The overall size of this antenna is 0.9 mm $\times 0.7$ mm $\times 0.1$ mm. It resonates at a frequency of 119.79 GHz, with a reflection coefficient (S11) of less than minus 10 dB throughout the resonant frequency range (S11 reflection coefficient of -21.36 dB), a bandwidth of 3.11 GHz, VSWR of 1.18, gain of 7.9 dB, and efficiency of 99.5%.

Keywords THz · 120 GHz · Microstrip patch antenna · Slot · HFSS

1 Introduction

Terahertz (THz) waves define the range of the electromagnetic wave spectrum between 20 and 0.1 THz, which corresponds to wavelengths between 15 and 3000 µm. Figure 1 shows this spectrum as a function of frequency and wavelength. The THz band is bounded there by the purple square, which extends from radio waves

S.-E. Didi (✉) · Y. Balboul · S. Mazer · M. EL Bekkali
IASSE Laboratory, Sidi Mohamed Ben Abdellah University, Fez, Morocco
e-mail: salaheddine.didi@usmba.ac.ma

I. Halkhams
LSEED Laboratory, UPF, Fez, Morocco

M. Fattah
IMAGE Laboratory, Moulay Ismail University, Meknes, Morocco

S. Das
Department of ECE, IMPS College of Engineering and Technology, Azimpur, W.B., India
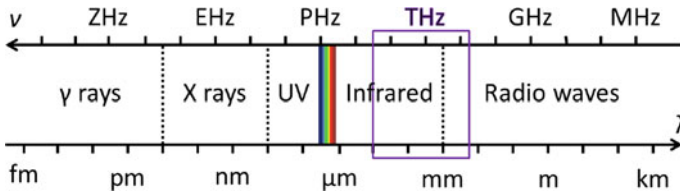
Fig. 1 Representation of the spectrum of electromagnetic waves as a function of frequency and wavelength. The purple frame delimits the THz domain

in the electrical band (<0.1 THz) to infrared waves in the optical band (>20 THz). The THz range covers a spectral area of great interest for many uses in spectroscopy, imaging, and telecommunications [1].

The development of THz spectroscopy began in the late 1980s with the time-domain spectroscopy (TDS) technique [2]. For example, it allows the identification of absorption lines of the polar molecule of water corresponding to the excitation of molecular rotations [3] or the absorption due to phonons or free carriers in metals or doped semiconductors.

Among the most common applications of THz spectroscopy is in the pharmaceutical industry. This application exploits the fact that the absorption lines of water are very well defined and more easily identified in the THz domain than in the optical spectrum [3]. Thus, the presence of water in pharmaceutical products can be identified during the control of a pharmaceutical process [4].

Like X-rays, THz waves have a high penetrating power. They can penetrate plastic and clothing fabrics, for example. Thus, they can be used to make deep images. However, unlike X-rays, THz waves only partially penetrate metals or skin. On the other hand, they have the advantage of being low energy, so they do not ionize the skin and allow body imaging without damaging cells.

These properties offer a great potential to THz sources, which are used for different needs: insecurity [5], industry [6], medicine [7], or art [8].

Telecommunications are an example. The bandwidth of radio waves is limited to 10% of the carrier frequency, which is 10 GHz [1], which limits the data transmission rate. However, by using a higher frequency wave, such as THz waves, the bandwidth is increased, which allows increasing the data rate transmitted by a wireless network.

In the terahertz frequency range, the most commonly used antennas are planar are the planar type and the dipoles (Hertz dipoles) built monolithically on the substrate. On this substrate are active components for radiation generation or detection with a hemispherical silicon lens placed on the backside of this substrate. Even though these antennas are not really "broadband", they have so far provided the best results in pulsed Terahertz spectroscopy. However, on the other hand, their poor efficiency makes them unsuitable for use in continuous operation, where the powers involved are low.

In this chapter, we present a design of a rectangular patch antenna with a rectangular-shaped groove, suitable for the terahertz operating frequency. The structure of this antenna is 0.9 mm × 0.7 mm × 0.1 mm. This paper is structured as

follows: The first step presents a general introduction of this paper, the second step is devoted to the different applications related to Terahertz frequencies, the third step presents the Terahertz radiation sources, the fourth step is devoted to the design of a Terahertz slot patch antenna, finally, the fifth step ends with a conclusion.

2 Applications of Terahertz Frequencies

A. Biomedical

Currently, different medical imaging techniques coexist. The first X-ray images were made in 1895 by Wilhelm Rontgen. A century later, the first demonstrations of imaging using terahertz frequency waves were performed [9]. X-ray imaging uses photons with quantum energies above a hundred eV, whereas in the terahertz range the energy is less than 1 eV (see Fig. 2). Since molecular ionization requires several eV, terahertz waves can currently be considered as non-ionizing electromagnetic radiation. However, the strong absorption of terahertz waves by water molecules and the high water content of the human body limit the applications of terahertz imaging to surface examinations.

Initially, the applications were focused on the examination of the skin. The control of the water content of the cells on the surface allows the detection of a deterioration of the skin. In the case of skin cancers, the use of terahertz imaging allows the early detection of this type of cancer undetectable by X-rays but also to monitor their evolution. In the case of wounds and burns, this detection can be used to evaluate the extent of the deterioration but especially to control the state of healing of the skin without removing the dressings [10]. As skin cancer is one of the most common cancers, its early detection is a significant advance in the biomedical field.

More specific applications have been demonstrated, notably in dentistry. Dentin has different water contents when it is healthy or not. This variation makes it possible to detect the depth of evolution of a cavity or the presence of dental tumors [11] while limiting the use of X-rays. These specific applications may allow an improvement of the current systems on X-ray exposure. Proofs of concept are a first step toward the democratization of these systems.
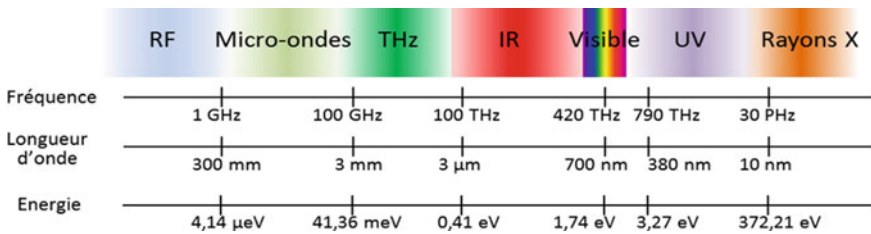

Fig. 2 Electromagnetic spectrum ($\lambda = c/f$; $E = hf$)

Early detection of plantar perforation disease or diabetic foot syndrome was the subject of a proof of concept in 2017 [12]. Thus, detection of arch dehydration, caused by vascular and neurological deterioration, can prevent susceptibility to this syndrome affecting people with diabetes. It could help avoid the amputation required in 15% of cases. The coupling of this type of imaging with other medical techniques increases the scope of application of these frequencies, in particular with endoscopy systems to visualize colon cancer cells [13].

The terahertz domain also has applications in biomedical research. In particular, terahertz spectroscopy allows the non-destructive analysis of tumors in vitro but also the analysis of nerve cells to improve the understanding of neurodegenerative diseases [14]. Biomedical studies using terahertz spectroscopy are now increasingly common in the research field but remain marginal in industry. The use of terahertz waves in the biomedical field contributes to the analysis of the human body and the establishment of medical diagnoses. Proofs of concept for these applications are essential elements for their deployment.

B. **The industry**

The propagation of terahertz waves in different media presents absorption and reflection spectra unique to each medium. This characteristic makes it possible to identify and differentiate each molecule, which is used for spectroscopy. Thus, opaque media in the visible range is transparent for specific THz frequencies. This advantage, applied to non-destructive testing, is of great interest to the industry. The reduction of terahertz waves allows determining the spectra associated with the absorption of products and consequently, their composition or their thickness.

The quality control of a product allows guaranteeing that it fulfills the desired functions. It can be divided into two types of inspection, destructive and non-destructive. In the majority of the mass distribution industries listed in Table 1, the inspection of a percentage of the elements of a batch is sufficient to guarantee the quality of all the elements of the batch. Thus, destructive quality control results in financial losses

Table 1 Industrial applications of non-destructive testing at terahertz frequencies

Sector	Principle
Alimentary	E-coli contamination, underpack control, quality control, fruit deterioration, genetically modified food, product origin presence of insects, plastic, presence of insecticide
Armory	Deteriorations, micro-cracks
Automotive	Degraded paint
Building	Cracks in cement under the plaster, thermal properties of walls
Pharmaceutical	Quality control
Photovoltaic	Local conversion efficiency
Plastic	Thickness of plastic bottles
Semiconductor	Lithography control package control, defect control during axial epic growth, counterfeit detection

depending on the percentage applied. Terahertz imaging in the industry finds its main applications in non-destructive testing which allows the use of the analyzed parts. This type of control is very attractive because of the financial advantage it offers. The cost of the inspection equipment is a key point since it must be lower than the financial losses estimated for destructive inspection. Some sectors, such as nuclear, construction, or space, produce a more limited volume of parts whose manufacturing cost is higher. The criticality of action in these sectors requires 100% control of the parts produced, non-destructive testing is therefore essential.

C. **Security and defense**

Spending in the security and defense sector in France was 32.7 billion euros in 2017. Two points must be dissociated, the security of citizens and the defense of the territory.

The observation of the French airspace by the radars contributes to the defense of the territory. The detection of an object by radar is possible when the waves emitted by the latter are reflected. Their attenuation makes it possible to determine the distance, speed, and size of the detected object. The use of coatings on moving objects, absorbing over a wide range of frequencies, limits the radar systems capable of detecting them. Thus, as coatings evolve, the frequency ranges used by radars are adjusted. Currently, the lack of terahertz sources limits their use, but a major issue for defense is the increase in the frequency of radar systems [15].

The ability of terahertz waves to image optically invisible elements is a considerable advantage for the security of citizens. For example, determining the contents of a package, envelope, or suitcase without opening it by using terahertz waves guarantees the safety of the control agents. The absorption spectra of drugs, explosives, and chemical agents are studied by the scientific community to realize security scanners applied to containers or individuals [16]. These scanners allow the detection of weapons concealed under clothing by THz cameras and increase security in public places.

Another aspect of security is that of the communications channels. Terahertz beams can be directional and point-to-point terahertz communications limit the possibility of intercepting the signal by an unauthorized person. Marginal use of terahertz waves limits the ability to properly receive the signal and thus increases the security and privacy of communications. More specific examples are developed, in particular, to contribute to the complexity of counterfeit money [17] by applying a resin patch on banknotes that can be deciphered by terahertz spectroscopy.

D. **Telecommunications**

The rate carried by optical fibers reaches Pb/s in the laboratory. But the lack of optoelectronic converters supporting these speeds limits the bandwidths currently used. In recent years, the growth in the number of connected objects predicts the saturation of Wi-Fi. Eldholm's law predicts a convergence of the necessary data rates in wired, nomadic, and wireless networks by 2030 [17]. Notably, improved video quality goes hand in hand with a need for higher throughput. Currently, devices associated with 4 K are being deployed and 8 K displays are available for purchase.

4 K requires 6 Gbps. A format in development called Super High Vision requires 24 Gbps illustrating this growth in throughput needed shortly. The occupation and allocation of the frequency bands currently in use limit the available frequency bands. An increase in carrier frequencies to terahertz frequencies increases the width of the frequency bands and represents a solution to the growing data rate demand.

Terahertz frequencies are for now not exploited and not assigned above the 275 GHz frequency band. Therefore the range of frequency comprised around the frequency of 275 GHz and 1 THz is possible to set up high-speed data communications. The losses seen at the heart of the atmosphere are due to the frequency of the scattered waves [18, 19] as well as to the peaks of the resonance peaks of all the chemical components that compose it. The movement of water molecules causes several absorption peaks in the terahertz band, but certain frequency ranges can be used and are presented in Table 2. The frequencies above 1 THz are not classified because of numerous peaks associated with phenomena called absorption that renders these frequencies unacceptable for high-speed and long-range communications. The loss suffered by terahertz waves through the atmosphere implies that we need robust and compact terahertz sources for use in actual environments.

Ultrafast non-wireless communications will likely require both low-range and long-range data transfers. Indeed, these very short-distance transmissions have various properties in electronic systems that are very applicable to them. Frequency increases have a significant effect on the amount of loss incurred when information flows through electrical circuits, increasing energy demand, and phenomena related to thermal effects while reducing device characteristics. Wireless communication distances sometimes reaching centimeters, combined with high data transmission rates and short "wireline" type links can replace the electrical interconnections employed within systems running in the multi GHz range [20].

Wireless communication systems that have very high data rates and low data carriers over short lengths of less than a meter make it possible to quickly download data, like magazines or HD movies, past a download kiosk. By augmenting the coverage length to a distance between 1 and 100 m and more, these uses are likely to involve a ward or apartment containing environmentally isolated transmission paths [21]. The scientific literature also mentions the possibility of achieving data transfers at rates ranging from 100 to 120 Gbps [22]. The distance needed to achieve these

Table 2 Usable frequency bands for wireless communications up to 1 THz

Frequency band (GHz)	Bandwidth (GHz)	Attenuation
215–315	100	2 à 4 dB/km
330–365	35	5 dB/km
390–435	45	9 dB/km
450–515	65	11 à 12 dB/km
625–725	100	11 dB/km
790–900	110	12 dB/km
925–950	25	15 dB/km

Fig. 3 Report on
non-wireless
communications operating in
the 60 GHz–1 THZ
frequency range for data
transfer rates above 1 Gigabit
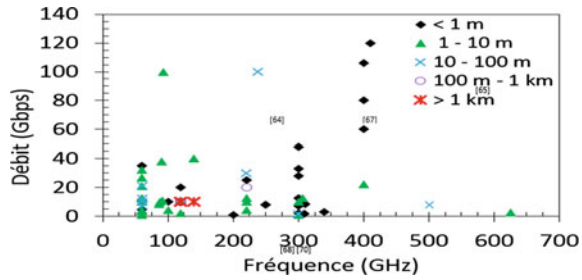
objectives can be estimated as 0.5 to 20 m. Figure 3 shows the results obtained in
the field of wireless communications, at a frequency of 60 to 1 THz.

The main link network is essentially made up of non-wireless communications
covering a larger area of more than a hundred meters and allowing for large trans-
mission flows with considerable data rates. The progressive development of this type
of grid consists in compensating for the change from microwave fireplaces to higher
frequency fireplaces. In a more distant future, and to meet the data and information
flow needs of users, we must consider a progressive evolution of the technology,
particularly in the direction of terahertz frequencies and sources. Scientific research
reports high performances reaching 10 Gbps at 120 and 140 GHz for distances
between 5.8 and 1.5 km [23].

## 3 Terahertz Radiation Sources

THz waves can be generated from different types of sources. We will describe here
the main ones:

- There are thermal sources that are based on black body radiation. The latter emits
  in the THz range at a very low intensity from 2 K [24]. For example, a mercury
  lamp has a spectrum extending over the entire THz range. However, its energy is
  low and the waves generated are incoherent.
- Electronic sources such as Gunn diodes, high-frequency transistors, and frequency
  multipliers allow the generation of a monochromatic wave up to 1 THz. We also
  note the existence of Backward Wave Oscillators (BWO), allowing to generate
  coherent fixed radiation of up to 2 THz.
- Quantum cascade lasers, based on inter-subband transitions in semiconductor
  quantum wells, allow the generation of monochromatic waves in the THz domain
  whose frequency depends on the semiconductor structure. The efficiency of these
  lasers is of the order of 10^{-5}, for generated powers of the order of a few milliwatts,
  and their tunability, which ranges from 1.2 to 4.9 THz [25], depends on the struc-
  ture of the semiconductor used. It should be noted that the design of a quantum
  cascade laser relies on the dimensions of the wells, which must have nanometric
  precision. This precision must be even finer for THz generation because the

inter-subband transition is made between two states very close in energy. There-
fore, the population inversion between the two sub-bands is very complicated to
realize experimentally. The same is true for tunability. Finally, quantum cascade
lasers generally operate at low temperatures [26], which limit their use for certain
applications.

- Gas lasers also allow the generation of a THz wave by optical pumping of gas
molecules. The latter presents a strong rotational transition in the THz domain
so that a laser transition between two vibrational levels and the emission of a
photon in the THz domain is possible. The most commonly used gases are CH_3F,
CH_3OH, NH_3, COOH, and CH_2F_2 [24]. They are commercially available. The
best efficiencies obtained with optically pumped gas lasers are of the order of
10^{-2}–10^{-3}, for generated powers of the order of 100 mW. Their emission can
range from 0.1 to 8 THz; each gas has its emission line. Gas lasers have three
major drawbacks. First, no tunability is possible because the generated spectrum
depends on the intrinsic properties of the gas used. Second, optical pumping must
be done at high wavelengths, around 9–11 µm, to excite the rotational energy
levels [24]. Finally, the combination of a pump laser and a gaseous amplifying
medium makes gas lasers very bulky sources.

- Optoelectronic sources are currently the most widely used for the generation of
a THz wave. It is a photo computer, also called "THz antenna". It consists of
two metallic electrodes separated by a few tens of microns and deposited on a
semiconductor substrate, as described in Fig. 4a [24]. The emission is based on a
DC bias current applied across the electrodes, so that the antenna behaves like a
capacitor in the circuit shown in Fig. 4b. An ultrashort infrared pulse, 20–200 fs,

Fig. 4 Schematic of a THz antenna (**a**) and equivalent RC circuit (**b**) [24]
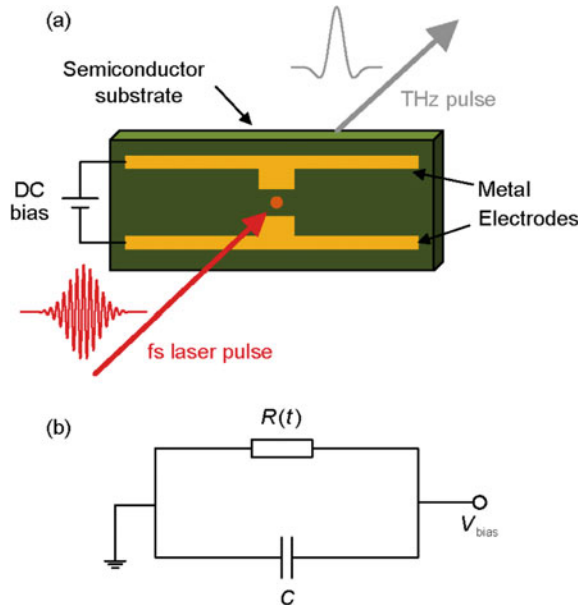
focused between the two electrodes closes the circuit for a short time. The sudden change of polarization current leads to the generation of THz radiation. An antenna generates a THz wave with a very broad spectrum, which can extend from 0.1 to 5 THz if very short femtosecond pulses are used. This results from the fact that a bias current is applied across the antenna electrodes, during the duration _t of the laser pulse. The shorter _t is, the wider the spectrum is, another important parameter is the carrier lifetime of the semiconductor used. The best conversion efficiencies are obtained in the laboratory with THz antennas; they are of the order of 10^{-2} [27].

- Finally, some sources generate a THz wave from a quadratic Frequency Difference Generation (FDG) process in a nonlinear crystal. Two visible or infrared laser optical fields create an induced polarization that generates a coherent electromagnetic wave in the THz domain. These sources are called "parametric sources". The maximum powers of these sources depend in part on the value of the optical damage threshold of the crystal. Two configurations are possible depending on whether the DFG is produced between two monochromatic laser pulses in the nanosecond regime or between two Fourier components within the same femtosecond laser pulse. In the first configuration, the THz source is monochromatic, in the second it is polychromatic.

4 Application

A. Procedure for designing a microstrip patch antenna

For the design of a microstrip patch antenna, we follow the following procedure. Firstly we choose the material needed for the printing that is to say the substrate in this document, we choose the Rubber_hard substrate with permittivity $\varepsilon r = 3$ and its height ($h = 0.1$ mm). Indeed the height of the substrate has a very important role concerning the general characteristics of microstrip antennas, the formula used to determine the maximum value of the substrate height has been established by the relationship of [28, 29]. In the second step, we determine the dimensions of the radiated element (patch) its width and length. In the third step, we also calculate the dimensions of the ground plane, and finally, we choose the type of power supply in this work we use the power supply by micro ribbon line, applying the formulas of [28] at 120 GHz.

$$E_s \leq \frac{0.3c}{2\pi f_{\text{res}} \sqrt{\varepsilon_r}} \tag{1}$$

$$W_p = \frac{c}{2 f_{\text{res}}} \sqrt{\frac{2}{\varepsilon_r + 1}} = \frac{\lambda}{2} \sqrt{\frac{2}{\varepsilon_r + 1}}$$

$$\varepsilon_{\text{eff}} = \frac{\varepsilon_r + 1}{2} + \frac{\varepsilon_r + 1}{2}\left(1 + 12\frac{E_s}{W_p}\right)^{\frac{-1}{2}} \tag{2}$$

$$L_{\text{eff}} = \frac{c}{2f_{\text{res}}}\varepsilon_{\text{eff}}^{-\frac{1}{2}} \tag{3}$$

$$\Delta L_p = 0.412\frac{(\varepsilon_{\text{eff}} + 0.3)\left(\frac{W_p}{E_s} + 0.264\right)}{(\varepsilon_{\text{eff}} - 0.258)\left(\frac{W_p}{E_s} + 0.8\right)} \tag{4}$$

$$L_p = L_{\text{eff}} - 2\Delta L_p = \frac{c}{2f_{\text{res}}\sqrt{\varepsilon_{\text{eff}}}} - 2\Delta L_p \tag{5}$$

$$W_g = W_p + 6E_s \text{ and } L_g = L_p + 6E_S \tag{6}$$

$$W_{\text{fed}} = \frac{2h}{\pi}\left[B - 1 - \ln(2B - 1) + \frac{\varepsilon_r - 1}{2\varepsilon_r}(\ln(B - 1) + 0.39 - \frac{0.61}{\varepsilon_r})\right] \tag{7}$$

$$B = \frac{60\pi^2}{z_c\sqrt{\varepsilon_r}} \tag{8}$$

$$L_{\text{fed}} = 3h, \ Z_C = 50 \ \Omega \tag{9}$$

$$|S_{11}|^2 = \frac{|Z_e - Z_c|^2}{|Z_e + Z_c|^2} \tag{10}$$

- E_s: the thickness of the substrate
- C: speed of light such that $c = 3 \times 108$ m/s
- f_{res}: resonance frequency
- ε_r: dielectric constant
- W_P: width of the patch
- L_p: length of the patch
- ε_{eff}: effective dielectric constant
- ΔL_p: the extension of the patch length
- L_g: the length of the ground plane
- W_g: width of the ground plane
- W_{fed}: the width of the feed line
- L_{fed}: the length of the feeder line
- S_{11}: return loss

The formulas in the above table were used to obtain the values of the different parameters that are presented in Table 3, that is to say, the overall sizes of the considered device. Figure 5 illustrates the structure obtained after calculating the dimensions of the various components of this antenna. The results obtained are used

Table 3 The parameters of the proposed antenna

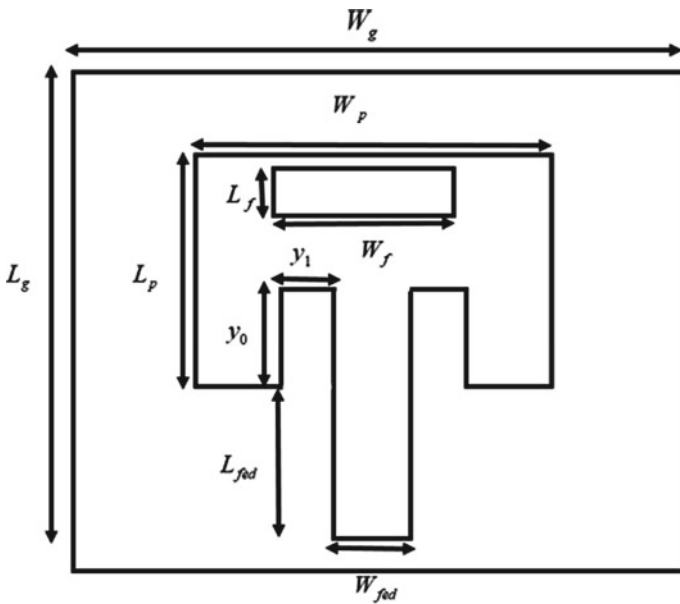| Parameters	Values (cm)
L_g	0.2
W_g	0.22
H	0.01
W_p	0.09
L_p	0.07
L_{fed}	0.093
W_{fed}	0.028
Y_0	0.071
Y_1	0.056
L_f	0.01
W_f	0.04

Fig. 5 Geometry of this proposed antenna

here to enhance the overall characteristics of this antenna, especially concerning its bandwidth and size reduction.

B. **Results of the simulations and discussions**

Figure 6 illustrates the result of the simulation of the reflection coefficient curve associated with the proposed antenna. This reflection coefficient S11 is used to check the matching properties provided by the antenna with a load or with a power cable.
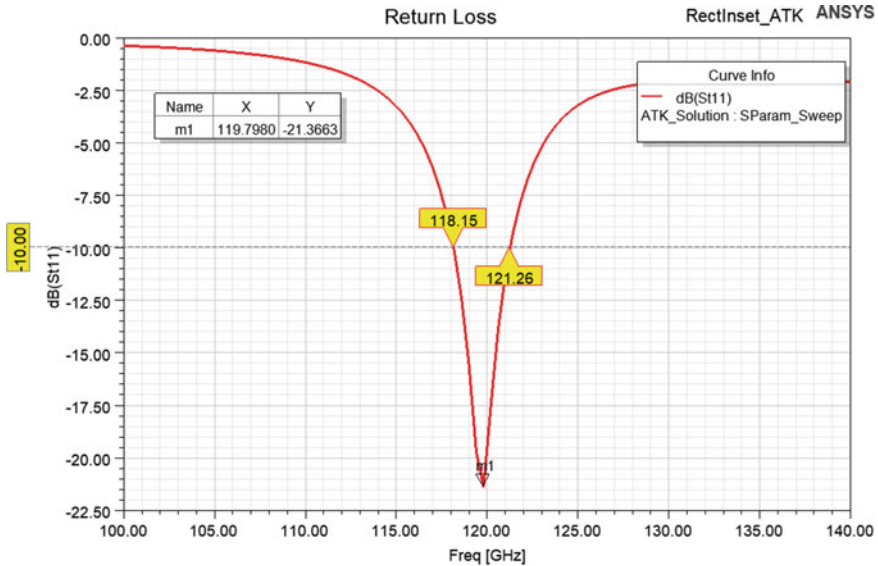
Fig. 6 Diagram of S11

The latter is related to both the input impedance Ze and that associated with the antenna load Zc. Its value is expressed in dB and is constantly negative. It simply corresponds to the relationship existing at the entry port. This relationship consists of the relationship between the reflected power and the incident power. Moreover, if the value of the reflection coefficient S11 < −10 dB it means that the exciting power is transmitted at 90%, which is the case of the designed antenna.

This antenna resonates at 119.79 GHz, with a reflection coefficient (S11) lower than minus 10 dB in the whole resonant frequency range, a bandwidth of 3.11 GHz, a gain of 7.9 dB. These results are validated by simulating the voltage standing wave ratio (VSWR) using the HFSS tool (see Fig. 7). The VSWR reflects the presence of standing waves in the transport cable attached to the electronic system in this case, namely an antenna. The VSWR is therefore obtained directly from the reflection coefficient. The standing wave ratio results from the phenomenon of reflection of a significant amount of the energy produced. This SWR must have a value between 1 and 2 within the bandwidth. Indeed this ratio must tend toward 1 when we want to maximize the power transmission of the antenna. As shown in Fig. 7 at the operating frequency of this antenna, we obtain the value of this SWR of 1.18.

The radiation pattern is a curve describing the radiation properties of antennas as a function of variations (θ, φ), that is to say in the polar plane. This radiation pattern can be in two-dimensional or three-dimensional form and is usually defined in the far field. The gain $G(\theta, \varphi)$, as well as the directivity, is parameters very close to each other, moreover, there is a related relationship between them, this one allows to determine the total efficiency of the antenna as $G(\theta, \varphi) = \eta D(\theta, \varphi)$ where η is the efficiency of the antenna, taking into account the losses in the conductors and
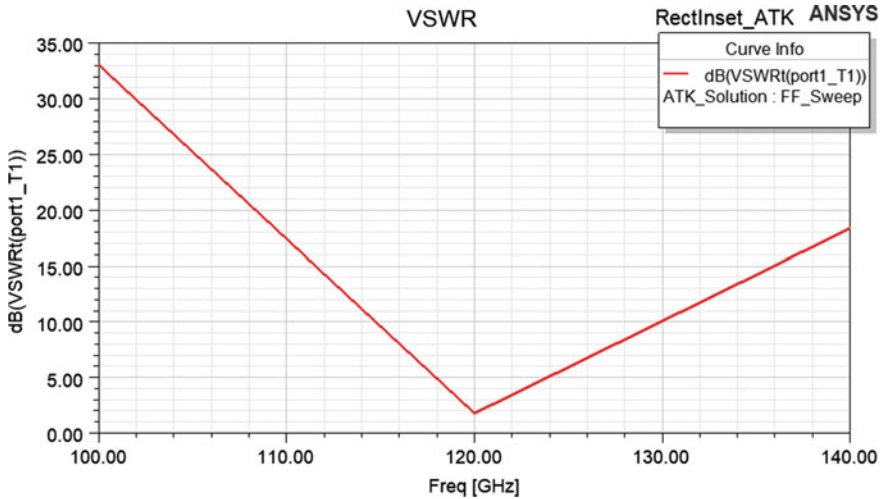
Fig. 7 Diagram of VSWR

dielectrics as well as the mismatch losses. Figure 8 shows the three-dimensional and two-dimensional gain patterns at 120 GHz for this examined microstrip patch antenna.

C. **Comparison of the results of this work with those obtained in the available literature**

In this section, we will compare the electrical performance of antennas in the terahertz frequency band, such as directivity, gain, reflection coefficient, VSWR, bandwidth, and efficiency of the proposed terahertz antenna with various existing works. The antenna [35] has a better reflection coefficient, VSWR, and bandwidth than the other papers, that is to say, the antennas [30–34] as well as the proposed antenna, as shown in Table 4. Antenna [31] has a very high bandwidth compared to antenna [30, 32–34], but its performance, such as gain and reflection coefficient, is low compared to
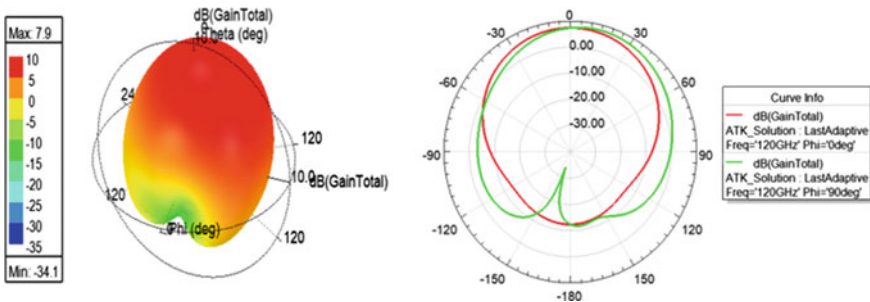

Fig. 8 The 3D and 2D gain pattern of this antenna suggests

Table 4 Comparison of the result of this antenna with the existing result

Refs.	Frequency band (GHz)	Directivity (dB)	VSWR	S11 (dB)	gain (dB)	Bandwidth (GHz)	Efficiency (%)
[30]	150–500	–	–	−16.23	5.17	2.2	–
[31]	960	–	1.3	−13.05	3.8	310	–
[32]	2.7	6.91	1.524	−13.66	6.59	90	92.9
[33]	0.750	5.71	–	−35	5.09	–	86.58
[34]	2.59	7.19	–	−35.183	5.03	–	60.8
[35]	6.994	7.408	1.0003	−75.66	7.286	386	97.21
Proposed	120	–	1.18	−21.36	7.9	3.11	99.5

antenna [30, 32–34]. Thus antenna [34] has a smaller efficiency than antenna [32, 33, 35] and the proposed antenna but offers a much better reflection coefficient than antenna [30–33] and the proposed antenna. While the proposed antenna achieves better results than the other antennas especially in terms of gain and efficiency. In addition, this antenna has a better reflection coefficient compared to antennas [31, 32] and its bandwidth is higher than that of the antenna [30] as shown in Table 4.

5 Conclusion

In this chapter, we present research concerning the THz frequency domain (more than 100 GHz) as well as applications related to terahertz frequencies and terahertz radiation sources. We design a two-slot microstrip patch antenna for the terahertz domain with an operating frequency of 120 GHz. In this chapter, we used the simulation software HFSS (High-Frequency Structure Simulator). The results obtained with this proposed antenna are remarkable with a small and compact size.

The simulation results obtained in this paper are reflection coefficient S11 = − 21.36 dB, the bandwidth of 3.11 GHz (from 185.15 GHz to 121.26 GHz), standing wave ratio VSWR = 1.18, the gain of 7.9 dB, and efficiency of 99.5%. This antenna applies to the terahertz frequency range.

References

1. D. Guillaume, S. Pascal, P. Fabio, P. Emilien, Z. Mohammed, B. Denis, B. Alexandre, A. Tahsin, L. Jean-François, L. Jean-François, THz communications using photonics and electronic devices: the race to data-rate. J. Infrared, Millimeter TeraHertz Waves **36**, 198–220 (2015)
2. J. Valdamis, G. Mourou, C. Gabel, Subpicosecond electrical sampling. IEEE J. Quantum Electron. **19**(4), 664–667 (1983)

3. E. Martin van, C.H. Fattinger, D. Grischkowsky, Terahertz time-domain spectroscopy of water vapor. Opt. Lett. **14**(20), 1128–1130 (1989)
4. H.-B. Liu, Y. Chen, X.-C. Zhang, Characterization of anhydrous and hydrated pharmaceutical materials with THz time-domain spectroscopy. J. Pharm. Sci. **96**(4), 927–934 (2007)
5. Y.C. Shen, T. Lo, P.F. Taday, B.E. Cole, W.R. Tribe, M.C. Kemp, Detection and identification of explosives using terahertz pulsed spectrocopic imaging. Appl. Phys. Lett. **86**(241116), 1–3 (2005)
6. O. Frank, Z. Wissem, B. Rene, M. Carsten, J. Joachim, R. Benoit, G. Jean-Paul, M. Patrick, V. Wouter, B. Pablo Venegas, G. Laura Vega, L. Ion, E. Rafael Martinez, S. Yehuda, V. Marijke, Aeronautics composite material inspection with a terahertz time-domain spectroscopy system. Opt. Eng. 53(3), 1–14, 031208 (2014)
7. P. Jae Yeon, C. Hyuck Jae, N. Gi-Eun, C. Kyoung-Sik, S. Joo-Hiuk, In vivo dual-modality terahertz/magnetic resonance imaging using superparamagnetic iron oxide nanoparticles as a dual contrast agent. IEEE Trans. Terahertz Sci. Technol. **2**(1), 93–98 (2011)
8. J.-P. Guillet, M. Roux, K. Wang, X. Ma, F. Fauquet, H. Balacey, B. Recur, F. Darracq, P. Mounaix. Art painting diagnostic before restoration with terahertz and millimeter waves. J. Infrared, Millimetre TeraHertz Waves 38(4) (2017)
9. B.B. Hu, M.C. Nuss, Imaging with terahertz waves. Opt. Lett. OL **20**(16), 1716–1718 (1995)
10. G. Yuan, Z. Reza, Millimeter wave reflectometry and imaging for noninvasive diagnosis of skin burn injuries. IEEE Trans. Instrum. Measur. **66**(1), 77–84 (2017)
11. J.S. Karsten et al., All-optoelectronic continuous-wave THz imaging for biomedical applications. Phys. Med. Biol. **47**(21), 3743 (2002)
12. G.G. Hernandez-Cardoso et al, Terahertz imaging for early screening of diabetic foot syndrome: a proof of concept. Sci Rep **7**, févr (2017)
13. D. Pallavi, A. Karim, C.S. Joseph, R.H. Giles, Terahertz polarization imaging for colon cancer detection. in *Millimeter, and Submillimeter-Wave Technology and Applications VII* ed by, R.F Terahertz, **8985**, 89850K (2014)
14. B. Tyler, C. Tanny, K. Kamrul, W. Jingxian, C. Avishek, R. Narasimhan, B. Keith, O.E. Magda, Pulsed terahertz imaging of breast cancer in freshly excised murine tumors. JBO, JBOPFO, **23**(2), 026004, févr (2018)
15. M.G. Thomas, C.D. Jason, W. Jerry, E.N. William, 1.56-THz compact radar range for W-band imagery of scale-model tactical targets. *Algorithms Synthetic Aperture Radar Imagery VII* **4053**, 615–623 (2000)
16. O.A. Maryam, M.S. Raed, R.R. Nadeen, A. Ghadah, Terahertz spectroscopy and imaging for the detection and identification of illicit drugs. 2017 Sens. Netw. Smart Emerg. Technol. (SENSET) 1–4 (2017)
17. H.J. Shin, M.-C. Lim, K. Park, S.-H. Kim, S.-W. Choi, G. Ok, Invisible security printing on photoresist polymer readable by terahertz spectroscopy. Sensors **17**(12), 2825, déc (2017)
18. B.J. Puttnam et al., 2.15 Pb/s transmission using a 22 core homogeneous single-mode multi-core fibre and wideband optical comb. in *2015 European Conference on Optical Communication (ECOC)*, 1–3 (2015)
19. A.S. Gustavo, R. Jose Manuel, G.P. Padro, Atmospheric attenuation in wireless communication systems at millimeter and THz frequencies [wireless corner]. IEEE Antennas Propag. Mag. **57**(1), 48–61, févr (2015)
20. G. Thierry Le, M. Pierre-Marie, A 45-GHz wireless transmission for a wireless interconnect network-on-board. in *2017 IEEE 21st Workshop on Signal and Power Integrity (SPI)*, 1–2 (2017)
21. P. Vitaly, K. Joonas, M. Dmitri, L. Janne, K. Yevgeni, J. Markku, Last meter indoor terahertz wireless access: performance insights and implementation roadmap. arXiv:1708.02963 [cs], août (2017)
22. S. Koenig et al., Wireless sub-THz communication system with high data rate. Nature Photonics **7**(12), 977–981 (2013)
23. W. Cheng, L. Changxing, C. Qi, L. Bin, D. Xianjin, Z. Jian, A 10-Gbit/s wireless communication link using 16-QAM modulation in 140-GHz band. IEEE Trans. Microwave Theory Tech. **61**(7), 2737–2746 (2013)

24. K. Zhong, W. Shi, D. Xu, P. Liu, Y. Wang, J. Mei, C. Yan, S. Fu, J. Yao, Optically pumped terahertz sources. Sci. China Technol. Sci. **60**(12), 1801–1818 (2017)
25. S.V. Miriam, S. Giacomo, W. Benjamin, D.N. Paolo, Quantum cascade lasers: 20 years of challenges. Optics Express **23**(4), 5167–5182 (2015)
26. B. Mikhail, C. Federico, New frontiers in quantum cascade lasers: high-performance room temperature terahertz sources. Phys. Scripts **90**(118002), 1–13 (2015)
27. Y. Shang-Hua, R.H. Mohammad, W.B. Christopher, J. Mona, 7.5photoconductive emitters with three-dimensional plasmonic contact electrodes. IEEE Trans. Terahertz Sci. Technol. **4**(5), 575–581 (2014)
28. D. Salah-Eddine, H. Imane, F. Mohammed, B. Younes, M. Said, E. Moulhime, Design of a microstrip antenna two-slot for fifth generation applications operating at 27.5 GHz. in *Springer International Conference on Digital Technologies and Applications(ICDTA), Lecture Notes in Networks and Systems, Fes, Morocco* **211**, 1081–1089 (2021)
29. E. Abdelhafid, A. Maryam, F. Mohammed, M. Said, E. Moulhime, A 5G mm-wave compact voltage-controlled oscillator in 0.25 µm pHEMT technology. Int. J. Electr. Comput. Eng. (IJECE) 11(2), 1036–1042 (2021)
30. R. Bhatoa, E. Sidhu, Novel terahertz microstrip patch antenna design for detection of biotin applications, in *2017 International Conference on Big Data Analytics and Computational Intelligence (ICBDAC)* (2017), pp. 289–292
31. A. Singh, S. Singh, A trapezoidal microstrip patch antenna on photonic crystal substrate for high-speed THz applications. Photonics Nanostruct. Fundam. Appl **14**, 52–62 (2015)
32. R. Bala, A. Marwaha (2015) Development of computational model for tunable characteristics of graphene-based triangular patch antenna in THz regime. Springer J. Computat. Electr. ISSN : 1569–8025, indexed by SCI, Thomson Reuter Journal list, Impact Factor 1.520, https://doi.org/10.1007/s10825- 015-0761-6, Print ISSN 1569-8025, Online ISSN 1572-8137, pp 1.6, online 2015
33. S.S. Anand, D.S. Kumar, R.J. Wu, M. Chavali, Graphene nanoribbon based terahertz antenna on polyimide substrate, Optik. Sci. Direct **125**, 5546–5549 (2014)
34. S. Mrunalini, A. Manoharan, Dual-band re-configurable graphene-based patch antenna in terahertz band for wireless network-on-chip applications. IET Microwaves, Antennas Propag. **11**(14), 2104–2108 (2017). https://doi.org/10.1049/iet-map.2017.0415
35. M.A.K. Khan, M.I. Ullah, R. Kabir et al., High-performance graphene patch antenna with superstrate cover for terahertz band application. Plasmonics **15**, 1719–1727 (2020). https://doi.org/10.1007/s11468-020-01200-z